Available online at www.sciencedirect.com
SCIENCE DIRECT®
Journal of Computational Physics 194 (2004) 256–277
JOURNAL OF COMPUTATIONAL PHYSICS
www.elsevier.com/locate/jcp

A hybrid continuum/particle approach for modeling subsonic, rarefied gas flows

Quanhua Sun [a,*], Iain D. Boyd [a], Graham V. Candler [b]

[a] Department of Aerospace Engineering, University of Michigan, Ann Arbor, MI 48109, USA
[b] Department of Aerospace Engineering and Mechanics, University of Minnesota, Minneapolis, MN 55455, USA

Received 23 June 2003; received in revised form 18 September 2003; accepted 18 September 2003

Abstract

A hybrid approach that combines a continuum approach solving the Navier–Stokes equations and a particle method called the information preservation (IP) method is implemented to simulate subsonic, rarefied gas flows accurately and efficiently. The coupling between the continuum and particle approaches relies on a continuum/particle interface, which is investigated in detail. The IP method preserves information at the macroscopic level that allows the continuum approach to directly use the information from the particle region. In order to correctly generate particles from the continuum region, two strategies are proposed. One strategy adopts a Marshak-type condition, which requires many particles in a cell to control the flux fluctuation due to the microscopic motion of particles. In the second strategy, reservoir cells and buffer cells are used, and this is the approach adopted in our general hybrid scheme. The location of the interface is determined using a continuum breakdown parameter. Studies show that the continuum breakdown parameter suggested by Garcia et al. can be used to determine the location of the interface, but the implementation of the interface also affects the location of the interface. Simulation of a flow over a flat plate shows the performance of the hybrid approach and reveals the effects of the cutoff value to a continuum breakdown parameter. This approach is also applied to study the aerodynamics of a micro-scale airfoil, which is very difficult for a single method. The hybrid approach generally spends less computational time than the IP method for rarefied gas flows, and the numerical performance of the hybrid approach depends on the number ratio of continuum cells to particle cells.

AMS: 65C20; 76P05; 76G99

Keywords: Hybrid approach; Information preservation method; Direct simulation Monte Carlo method; Rarefied gas dynamics; Subsonic gas flow

1. Introduction

Many problems of current interest involve flow fields in the transitional regime. Examples include gas flows in and around micro-electro-mechanical systems (MEMS) [1,2] and the aerothermodynamics of

* Corresponding author. Tel.: +1-734-764-7479; fax: +1-734-763-0578.
E-mail address: qsun@engin.umich.edu (Q. Sun).

0021-9991/$ - see front matter © 2003 Elsevier B.V. All rights reserved.
doi:10.1016/j.jcp.2003.09.005

hypersonic vehicles [3]. These flows are comprised of continuum and rarefied regions, and thus they belong to multi-scale flows. Hence, methods designed for one scale are not suitable to simulate these flows in terms of physical accuracy and numerical efficiency. An efficient approach is therefore to combine the numerical efficiency of continuum approaches for the continuum region and the physical accuracy of kinetic approaches for the rarefied region.

Continuum methods are relatively mature and have been widely applied to flows in the continuum regime [4]. These methods can also be applied to flows in the slip regime if proper slip boundary conditions are adopted [5]. Continuum methods, however, cannot predict flows in the transitional regime because of the physical limitation of continuum equations [6]. Then, kinetic approaches must be applied where continuum equations are not valid. However, kinetic approaches, such as the direct simulation Monte Carlo (DSMC) method [7], are generally several orders of magnitude more numerically expensive than continuum methods, especially for flows in the continuum regime. Therefore, it is highly desired to develop hybrid techniques that can reduce the computational cost of a numerical simulation by limiting a kinetic method to the regions where kinetic equations must be applied, and use a continuum method in the rest of the computational domain.

In the past 10 years, many studies of hybrid techniques have been reported [8–24]. There exist weakly coupled schemes [8,9] for which an initial continuum solution on the entire computational domain provides a boundary condition for a particle method that is applied only to the rarefied domain. There are also overlapping coupling strategies for which a local particle method provides a wall boundary condition for a global continuum scheme [10], or even provides transport coefficients for a continuum method [11]. However, non-overlapping coupled schemes may give better performance for accuracy and efficiency. Wadsworth and Erwin first demonstrated such a scheme by simulating one-dimensional (1-D) shock waves [12] and considering two-dimensional (2-D) slit flows [13] using a property extrapolation technique to couple a Navier–Stokes (N–S) scheme and the DSMC method through an interface. Aiming to investigate possible coupling techniques, Hash and Hassan [14] performed detailed studies of a hybrid code and suggested that the Marshak condition (half fluxes from both sides are summed to be the full flux through the interface) is a preferred coupling technique. However, in a later paper, Hash and Hassan [15] pointed out that the large statistical scatter associated with the DSMC method precluded the application of the Marshak condition to low-speed flows. For further development of hybrid methods, adaptive hybrid schemes are proposed. Roveda et al. [16] described an Euler/particle approach that can analyze unsteady flows by coupling an adaptive discrete velocity (ADV) Euler solver and the DSMC method with an adaptive interface. In a following paper, Roveda et al. [17] successfully simulated an unsteady pressure driven slit flow with this scheme. There are other hybrid schemes for different problems in the literature, including the hybrid Boltzmann/N–S approach for analyzing hypersonic flows by Tallec and Mallinger [18], the adaptive mesh and algorithm refinement (AMAR) method by Garcia et al. [19], the hybrid atomistic-continuum approach by Hadjiconstantinou [20] and the combined continuum/DSMC technique for studying microfluidics filters by Aktas and Aluru [21].

Most of the hybrid schemes, however, exhibit statistical scatter difficulties with the particle methods. Sampling a large number of particles is generally adopted by most authors with multiple time steps [12,14,21], ghost cells [16], or local average from multiple cells [22]. Then a large sample size is required especially for low-speed flows, making it numerically expensive to couple two methods for every time step. As a result, for general rarefied gas flows, it is preferable to couple a kinetic method having a small statistical scatter with a continuum solver.

In this paper, a novel hybrid approach is developed for modeling subsonic, rarefied gas flows by coupling a particle approach called the information preservation (IP) method and a continuum approach solving the N–S equations. Because the IP method exhibits very small statistical scatter and has the macroscopic information available at any time, the IP method is strongly coupled with the N–S approach at each time step to have an adaptive hybrid approach. We organize the rest of the paper as follows. Section 2 summarizes

the IP method and the N–S approach. Section 3 discusses general physical issues and specific numerical issues of the hybrid approach. Section 4 provides some example results and discusses numerical performance of the hybrid approach. Finally, we end with some concluding remarks.

2. Description of the continuum and particle methods

2.1. The information preservation method

The IP method [25–27] is a recently developed particle method for modeling rarefied gas dynamics based on the DSMC method. The IP method simulates microscopic particles as in the DSMC method, but also solves information at the macroscopic level to obtain macroscopic flow information, which makes the IP method less numerically expensive than the DSMC method.

The DSMC method models a gas flow with representative particles in simulated physical space. The position coordinates and the velocity components (and the internal energy state) of the simulated particles are preserved and are modified with time as the particles are concurrently followed through representative collisions and boundary interactions. However, the inherent statistical scatter associated with the method requires a large sample size to obtain a smooth result, which makes the DSMC method numerically expensive, particularly for low-speed flows.

The IP method reduces the statistical scatter by additionally preserving flow information at the macroscopic level for the simulated particles and for the computational cells. The preserved information is modeled based on the transfer equation of the Boltzmann equation. For example, the transfer equation for momentum can be written as Eq. (1), and the preserved velocity of particle i is modeled according to Eq. (2).

$$\frac{\partial}{\partial t}\left(nm\overline{\mathbf{V}_i}\right) + \nabla\cdot\left(nm\overline{\mathbf{c}_i\mathbf{V}_i}\right) = -\nabla\cdot\left(nm\overline{(\mathbf{c}_i-\mathbf{V}_i)(\mathbf{c}_i-\mathbf{c}_0)}\right) = -\nabla p' + \nabla\cdot\boldsymbol{\tau}', \tag{1}$$

$$\frac{\partial}{\partial t}(nm\mathbf{V}_i) + \text{microscopic movement} = -\nabla p + \text{collisions}. \tag{2}$$

In Eqs. (1) and (2), $\mathbf{V}_i$ is the preserved velocity of particle i, $\mathbf{c}_0$ is the flow velocity, $\mathbf{c}_i$ is the microscopic velocity of particle i , n is the number density, m is the mass of gas molecules, p' and $\boldsymbol{\tau}'$ are the normal and shear stresses of the collision term in the transfer equation, respectively. The preserved information at the macroscopic level is initialized by the ambient flow condition or the inflow/outflow boundary condition. In every time step, particles are moved according to their microscopic velocity, then the preserved macroscopic information for particles is updated during collisions, and is modified to include the pressure effects excluded in the collisions. The preserved macroscopic information for cells is set as the average of the corresponding information for particles in the cell, because the particles in one cell come from different locations following their microscopic movements and thus have different preserved macroscopic information. In order to correctly model the shear stress and the heat transfer of a flow, an energy flux model for low-speed flows and a collision model were proposed for the preserved macroscopic information in the IP method [26]. In particular, an energy flux model is required because the energy flux of a flow is generally larger than the preserved energy transferred during the particle movement. Therefore, other flux models may be required for high-speed flows [28]. The validity of the IP method has been shown by many examples [2,25–27,29,30], including typical subsonic steady flows and low frequency unsteady flows ranging from the near-continuum regime to the free molecular regime.

The main benefit of the IP method is its relatively small statistical scatter compared with the DSMC method for modeling low-speed flows, which can greatly reduce the computational cost for these flows. Comparison of the statistical scatter obtained using the IP and DSMC methods is illustrated in Fig. 1, by

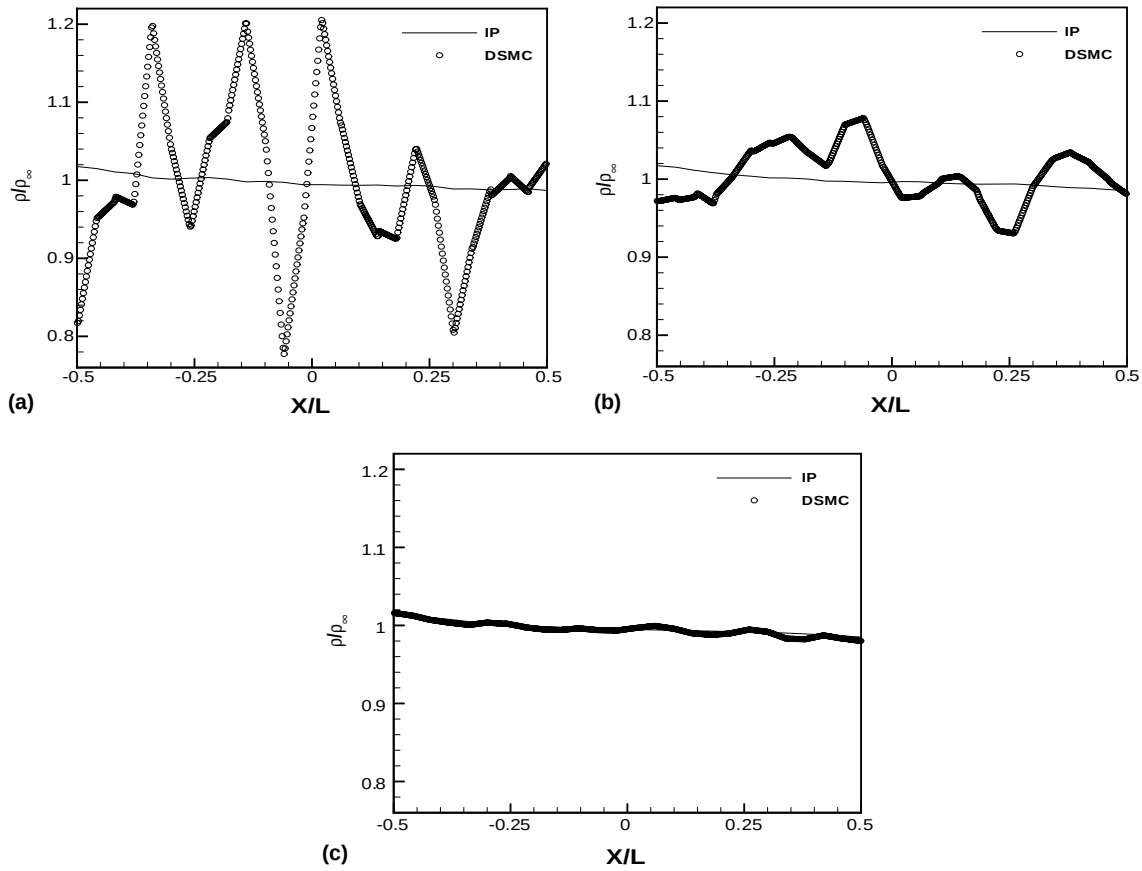

Fig. 1. Density profiles obtained using IP and DSMC methods along a straight line from a low-speed gas flow over a flat plate: (a) a sample size of 20 particles per cell with 1 time step; (b) a sample size of 20,000 particles per cell with 1000 time steps; (c) a sample size of 20,000,000 particles per cell with 1,000,000 time steps.

showing the density profile along a solid line from a low-speed air flow over a flat plate. Because the IP scatter is very small, traditional boundary treatments used in computational fluid dynamics [4], e.g., the characteristic boundary condition, can be used for the IP method, which circumvents some boundary condition issues for the DSMC method [31,32]. It also helps in the development of an efficient adaptive hybrid scheme.

2.2. The Navier–Stokes approach

The N–S equations are expressed in conservation form as follows:

$$\frac{\partial \mathbf{U}}{\partial t} + \nabla \cdot \left(\mathbf{F}_{\mathrm{o}} + \mathbf{F}_{\mu}\right) = 0, \tag{3}$$

where

$$\mathbf{U} = \begin{bmatrix} \rho \\ \rho \mathbf{u} \\ e \end{bmatrix}, \quad \mathbf{F}_{\mathrm{o}} = \begin{bmatrix} \rho \mathbf{u} \\ \rho \mathbf{u}\mathbf{u} + p\mathbf{I} \\ (e+p)\mathbf{u} \end{bmatrix}, \quad \mathbf{F}_{\mu} = \begin{bmatrix} 0 \\ -\boldsymbol{\tau} \\ -\boldsymbol{\tau} \cdot \mathbf{u} + \mathbf{q} \end{bmatrix}, \tag{4}$$

$$p = (\gamma - 1)\rho\varepsilon, \quad \varepsilon = e/\rho - \mathbf{u}\cdot\mathbf{u}/2, \tag{5}$$

$$\tau_{ij} = \mu\left(\frac{\partial u_i}{\partial x_j} + \frac{\partial u_j}{\partial x_i}\right) - \frac{2}{3}\mu\frac{\partial u_k}{\partial x_k}\delta_{ij}, \quad q = -\kappa\nabla\cdot T. \tag{6}$$

In the previous expressions, ρ is the mass density, $\mathbf{u}$ is the velocity vector, p is the pressure, and e is the specific total energy. In order to match the variable hard sphere (VHS) model [7] used in the IP method, the viscosity coefficient μ and the coefficient of thermal conductivity κ are expressed as follows:

$$\mu = \mu_0\left(\frac{T}{T_0}\right)^{\omega}, \tag{7}$$

$$\kappa = \frac{9\gamma - 5}{4\gamma - 4}R\mu, \tag{8}$$

where μ_0 is the viscosity coefficient at temperature T_0, ω is the viscosity temperature index in the VHS molecular model, and R is the specific gas constant.

In our hybrid approach, the continuum approach [33,34] solves the N–S equations using a finite volume formulation. The fluxes are evaluated with a second-order accurate modified Steger–Warming flux-vector splitting approach [33]. Namely, the fluxes are decomposed into an inviscid part and a viscous part as shown in Eq. (3). The inviscid fluxes are then split into components along the characteristic directions of the flow because the hyperbolic property of the fluxes allows upwind numerical approximations to be used for the spatial derivatives. The viscous fluxes are calculated using centered differences. A slip boundary condition is also implemented in the continuum approach with the use of the Maxwell-type slip velocity expression [35]:

$$u_s = \frac{2 - \sigma}{\sigma}\lambda\left.\frac{\partial u}{\partial n}\right|_w, \tag{9}$$

where σ is the accommodation coefficient, λ is the mean free path of the gas given by $\lambda = 2\mu/\rho\langle c\rangle$, and $\langle c\rangle$ is the mean molecular speed of the gas.

3. The hybrid continuum/particle approach

There are several physical and numerical issues in the development of a hybrid approach. We first discuss the physical issues for coupling a continuum method and a particle method, which includes the determination of the continuum/particle interface and the communication of information through the interface. We then describe the numerical issues of our novel hybrid approach.

3.1. Location of the continuum/particle interface

One key issue of a hybrid approach is how to divide the computational domain into particle and continuum domains. There are two criteria to determine the location of the continuum/particle interface. The first one is that both solvers must be valid to simulate the flow near the interface. The second one is that the continuum domain should be as large as possible in order to achieve the maximum numerical efficiency for the hybrid approach. Thus, the interface should be placed where the continuum equations tend to break down, because the IP method is valid for the entire computational domain for low-speed flows. Hence, a continuum breakdown parameter must be used to determine the interface location.

In principle, a continuum breakdown parameter can be derived from the relationship between the Boltzmann equation and the N–S equations. The N–S equations approximate the Boltzmann equation under near-equilibrium conditions. Hence, any approximation made to derive the N–S equations can be used to derive a continuum breakdown parameter, such as the Knudsen number (Kn). A general procedure to derive the N–S equations is to use Chapman–Enskog theory [36]. In this theory, the velocity distribution function is assumed to be in the form of the power series:

$$f = f^{(0)} + Kn \cdot f^{(1)} + Kn^2 \cdot f^{(2)} + \cdots \tag{10}$$

The first term $f^{(0)}$ is the Maxwellian distribution for an equilibrium gas, and an alternative form of the expression is

$$f = f_0(1 + \Phi_1 + \Phi_2 + \cdots) \tag{11}$$

The first-order solution of the distribution function can be expressed as follows:

$$f(\mathbf{C}) = f_0(\mathbf{C})(1 + \Phi_1(\mathbf{C})), \quad \mathbf{C} = \mathbf{c}/(2kT/m)^{1/2}, \tag{12}$$

$$f_0(\mathbf{C}) = \frac{1}{\pi^{3/2}} e^{-C^2}, \tag{13}$$

$$\Phi_1(\mathbf{C}) = (\mathbf{q}^* \cdot \mathbf{C})\left(\frac{2}{5}C^2 - 1\right) - \boldsymbol{\tau}^* : (\mathbf{CC}), \tag{14}$$

$$\mathbf{q}^* = -\frac{\kappa}{p}\left(\frac{2m}{kT}\right)^{1/2}\nabla T, \quad \tau^*_{ij} = \frac{\mu}{p}\left(\frac{\partial V_i}{\partial x_j} + \frac{\partial V_j}{\partial x_i} - \frac{2}{3}\frac{\partial V_k}{\partial x_k}\delta_{ij}\right). \tag{15}$$

It can be shown that the substitution of this solution into moment equations leads to the monatomic gas form of the N–S equations. Hence, the N–S equations cease to be valid when the higher order terms in the distribution function cannot be neglected. The magnitude of the coefficients in the first-order solution may indicate the validity of the N–S equations. Physically, the continuum equations break down when the velocity distribution function deviates from its equilibrium state by a sufficient degree. However, there is no theory that indicates how large the higher order terms in the power series should be or how far the distribution function should deviate from equilibrium for the N–S equations to be invalid. Hence, finding a general continuum breakdown parameter and its cutoff value is still an open research subject.

In the literature, several continuum breakdown parameters have been proposed, including Bird's parameter P [37], the gradient-length local Knudsen number Kn_{GLL} [38], Tiwari's criterion $\|\phi\|$ [39], and the parameter B [19]. These four parameters are as follows:

$$P = \frac{U}{\rho v}\left|\frac{\mathrm{d}\rho}{\mathrm{d}s}\right|, \tag{16}$$

$$Kn_{\mathrm{GLL}} = \frac{\lambda}{Q}\left|\frac{\mathrm{d}Q}{\mathrm{d}l}\right|, \tag{17}$$

$$\|\phi\| = \frac{1}{\rho RT}\left[\frac{2}{5}\frac{|q|^2}{RT} + \frac{1}{2}\|\tau\|^2_{\mathrm{E}}\right]^{1/2}, \tag{18}$$

$$B = \max\left\{\left|\tau^*_{ij}\right|, \left|q^*_{ij}\right|\right\}. \tag{19}$$

However, only the parameter P and the parameter Kn_{GLL} have been extensively investigated for simulating expanding jet flows and for simulating hypersonic compressible flows, respectively. The validity of these parameters for general flows is unclear, but all these parameters represent some kind of combination of the coefficients in the first-order Chapman–Enskog solution. Even if a parameter is acceptable for a certain type of flow, the cutoff value for the parameter is also difficult to determine. Some researchers investigate the cutoff value by computing the breakdown parameter when differences between a continuum solution and a kinetic result are larger than 5%, whereas some simply take a small number as the cutoff value. Generally, the cutoff value can only be determined by numerical tests, which means the cutoff value depends on the tolerance chosen for the difference between the hybrid solution and the kinetic result. It is also possible that the cutoff value is problem-dependent because different flow configurations vary in their physical behavior. Therefore, a conservative cutoff value should be used in applications of a hybrid approach.

In the present implementation of the hybrid approach, the continuum breakdown parameter B is selected to be the continuum/particle interface indicator because this parameter includes all the coefficients of the first-order Chapman–Enskog solution. However, parameter $\|\phi\|$ is very similar to parameter B in terms of the physical nature, and parameter $\|\phi\|$ is expected to work as well as parameter B . The effects of the cutoff value for the continuum breakdown parameter are illustrated in Section 4.

3.2. Coupling the continuum and particle methods

In our adaptive hybrid approach, the continuum domain and the IP domain are separated by a continuum/particle interface. Through the interface, the continuum and IP domains exchange information at every time step. Specifically, the IP method needs the interface to generate particles based on information from the N–S approach, whereas the N–S approach needs fluxes through the interface that requires information from the IP method.

For general hybrid approaches, the interface condition for the continuum approach is very difficult or expensive to obtain due to the large statistical scatter associated with the particle solver. However, as stated in Section 2.1, the IP method preserves the macroscopic information for cells that has very small statistical scatter (Fig. 1). Therefore, the continuum approach can directly use the macroscopic information preserved in the IP cells to evaluate the fluxes through the interface. Then the interface becomes internal edges to the continuum approach.

On the other side, the interface should provide particles for the IP method. In many hybrid approaches, the number of generated particles and their microscopic information are determined from half fluxes based on the macroscopic properties at the interface. However, it is only valid for equilibrium flows to sample the velocity for particles from a Maxwellian distribution. In order to have a larger continuum domain, it was suggested by Hash and Hassan [15] to sample the velocity of particles from a Chapman–Enskog distribution (Eqs. (12)–(15)). Furthermore, Garcia et al. [19] suggested to generate particles based on the local macroscopic information and its gradients. In the present hybrid approach, two different strategies are used to generate particles through the interface from the continuum domain.

In the first strategy, a condition similar to the Marshak condition [14] is used: the full fluxes crossing the interface based on the local macroscopic values are set to be the sum of the counted half fluxes from the IP side and the half fluxes from the continuum side that are to be determined. Details of this condition are shown in Eqs. (20)–(22), where f is the full flux, and subscripts p and c represent the particle and continuum sides, respectively.

$$N_c + N_p = \frac{f_\rho \cdot A \cdot \mathrm{d}t}{m}, \tag{20}$$

$$N_c \mathbf{V}_c + \sum_{j=1}^{N_p} \mathbf{V}_{p,j} = \frac{(\mathbf{f}_{\rho \mathbf{V}} - p\mathbf{n}) \cdot A \cdot dt}{m}, \tag{21}$$

$$N_c (e + 0.5V^2)_c + \sum_{j=1}^{N_p} (e + 0.5V^2)_{p,j} = \frac{(f_{\rho(e+0.5V^2)} - p\mathbf{V} \cdot \mathbf{n}) \cdot A \cdot dt}{m}. \tag{22}$$

These equations determine the number of generated particles N_c and the macroscopic information V_c , e_c (or T_c) for the generated particles, whereas the microscopic information for the particles is sampled from the Chapman–Enskog distribution based on the local macroscopic values [40]. Because particles cannot be generated as a fractional number, the number of generated particles is rounded to the nearest integer in the implementation. The difference of the half fluxes due to this rounding process is stored and is added to the next time step ensuring that the half fluxes from the continuum side are implemented correctly.

This strategy has been tested for several flows. It turns out that the coupling process works well when the number of simulated particles in each cell is not too small (more than 50 for 1-D flows and more than 200 for 2-D flows). However, the code may crash when there are not enough particles in the cells. This occurs because the determined macroscopic information preserved in the generated particles may have large fluctuations due to the rounding of the particle number flux and to the fluctuation of the number of particles leaving the particle domain. Therefore, this strategy should be reserved for flows when it is possible to use a large number of particles.

A second strategy is then developed to avoid directly generating particles through the interface. Near the interface, buffer and reservoir cells are used in the continuum domain as illustrated in Fig. 2. These buffer and reservoir cells are also treated as particle cells except that the macroscopic information for the cells is provided by the continuum solver. Therefore, the interface becomes internal cell edges for the IP treatment. Specifically, the reservoir cells provide particles that may enter the buffer cells or the IP domain, while the buffer cells are used to improve the represented information of particles that can enter the IP domain through the interface. The algorithm for this strategy is as follows:

(1) In the initialization step, particles are generated for the buffer cells. The Chapman–Enskog distribution is used to specify particle microscopic velocity, and a Boltzmann distribution is used to set the molecule internal energy, while all particles in the cell preserve the same macroscopic information for the cell.

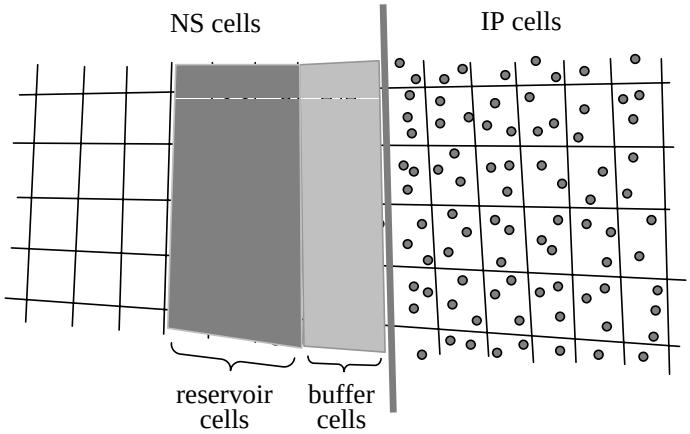

Fig. 2. Illustration of the interface and cell structures for the hybrid continuum/particle approach.

(2) During each time step, new particles are generated for the reservoir cells according to the same way for generating buffer cell particles.
(3) Particles in the buffer and reservoir cells are selected for collisions and motion using general IP procedures. A particle is removed when it enters a non-particle cell.
(4) After the collision and movement sub-steps, all particles in the reservoir cells are removed.
(5) Steps (2)–(4) are repeated until the simulation is finished.

It should be pointed out that all particles in a reservoir cell have the same preserved macroscopic information, which is only an approximation because there exist gradients of flow properties. This is why the buffer cells are used to improve the quality of particles that can enter the IP domain. Therefore, with this algorithm, using more buffer cells will improve the interface properties, but will increase the computational cost. Hence, only several levels of buffer cells are used. The number of reservoir cells is also determined such that only a negligible number of particles will enter a buffer cell from a continuum cell during one time step. Generally, two or more levels of reservoir cells are required. This second strategy works very well, as will be shown in Section 4.

3.3. Implementation of the continuum/particle interface

The continuum/particle interface is determined by the continuum breakdown parameter. Hence, the interface adjusts its location as the simulated flow develops with time. In order to track the interface, a mapping technique is used to mark the cells. A similar technique can be found in the work by Roveda et al. [16].

In the mapping technique, each computational cell is assigned a three-digit number to represent the type of a cell, which can be an IP cell, a reservoir cell, a buffer cell, or a continuum cell other than buffer or reservoir cell. The number is in the form of "$a + 10b + 100c$". Here, "a" indicates whether the cell is in the continuum domain (0) or the IP domain (1). "b" shows whether the cell is adaptive (0) or not (1), which means that cells can be forced to be of a fixed type. "c" is used to indicate the levels of buffer or reservoir cells, or to indicate the IP cells neighboring the interface. Fig. 3 shows a simple map that illustrates the cell types and the interface.

The algorithm for setting the cell type is as follows.

(1) Sweep all computational cells to determine "a" by comparing the cutoff value of the continuum breakdown parameter to its local value. The continuum breakdown parameter is time-averaged for steady simulations. If the local value is smaller than the cutoff value, the cell is determined as a continuum cell ($a = 0$). Otherwise, it is an IP cell ($a = 1$). In order to eliminate spurious, miniscule patches of continuum or particle domains, the neighbor survey approach [17] is used to smooth the interface. Generally, "b" does not change after it is initialized.
(2) Set "c" to 1 for all cells neighboring the interface.

10	10	0	0	0	0	0	0	0	0	0	0	0	0	0	0	10	10
10	10	0	0	0	0	0	0	0	0	0	0	0	0	0	0	10	10
10	10	0	0	0	0	0	200	200	200	200	200	0	0	0	0	10	10
10	10	0	0	0	0	200	100	100	100	100	100	200	0	0	0	10	10
10	10	0	0	0	200	100	101	101	101	101	101	100	200	0	0	10	10
10	10	0	0	200	100	101	1	1	1	1	1	101	100	200	0	10	10
10	10	0	200	100	101	1	11	11	11	11	1	101	100	200	0	10	10
10	10	0	200	100	101	1	11	11	11	11	1	101	100	200	0	10	10
10	10	0	200	100	101	1	11	11	11	11	1	101	100	200	0	10	10

Fig. 3. An illustrative map showing the cell types and the interface.

(3) Set "c" to $i+1$ for the continuum cells neighboring buffer cells or reservoir cells whose "c" is i $(i > 0)$ until the required levels of buffer and reservoir cells are marked.

3.4. Implementation of the hybrid approach

In the present hybrid approach, both the IP method and the N–S approach are implemented in the MONACO system [41], which was first developed by Dietrich and Boyd as a DSMC code. Because each computational cell may be handled by either solver, each cell has the information for both solvers, including the cell type, the continuum breakdown parameter, the density, the velocity, the temperature, the fluxes at each cell edge, and the particle information. The solver for a cell is chosen by the cell type that is determined by the continuum breakdown parameter. If the continuum approach is chosen, then the macroscopic information is evaluated based on the fluxes through each cell edge. Otherwise, the macroscopic information is updated using the particle information.

The algorithm of the implementation with our second strategy for generating particles through the interface is presented as follows:

(1) All necessary information for the simulation is initialized. Namely, the computational cells are defined and the cell type is initialized as desired. The macroscopic information for the cell is set according to the ambient condition. Then particles are distributed for the IP cells, the buffer cells, and the reservoir cells. During each time step, the following operations are executed.
(2) All particles collide and move similar to the usual IP code. When a particle reaches an open boundary or a continuum cell other than a buffer or reservoir cell, it is removed. New particles are injected at the open boundary, but no particles are generated from the continuum cell side.
(3) The macroscopic values for all cells are re-evaluated. All continuum cells including the buffer and reservoir cells update their values according to the N–S approach, whereas all IP cells sample the macroscopic information from the preserved information of the particles contained in the cell.
(4) Remove all particles in the reservoir cells because particles are to be re-generated.
(5) Calculate the continuum breakdown parameter for every cell and use the interface mapping algorithm to set the new cell type. Then generate particles for particle cells (including the buffer and reservoir cells) if there are no particles in the cell, and remove particles from the continuum cells (excluding the buffer and reservoir cells) that are occupied by particles. In many cases, it is not necessary to adjust the interface for every time step. Hence, a frequency for adapting the interface is also implemented in the code.

4. Results

The proposed hybrid approach is applied to simulate several subsonic, rarefied gas flows. In this section, a Couette flow is simulated using the hybrid approach with the first strategy of generating particles for the IP method from the continuum side, which shows the validity of the approach and helps evaluation of typical continuum breakdown parameters. The second strategy of generating particles is evaluated by an example of a flow over a flat plate. Using this example, the effects of several parameters are discussed. The approach is also used to investigate the aerodynamic characteristics of a micro-scale airfoil, which is impossible to be studied by a single method. We present results when the angle of attack is 20°. Finally, the numerical performance of the hybrid approach is discussed.

4.1. A Couette flow

Couette flow is well defined and is often used as a benchmark problem to evaluate a numerical scheme [8]. For the present investigation, this flow is used to assess the first strategy of generating particles through

the interface for the hybrid approach and to evaluate the validity of typical continuum breakdown parameters.

In the Couette flow, one of two parallel plates has a velocity of 300 m/s whereas the other is at rest. The temperature of both plates is kept at 273 K, and full momentum and thermal accommodation is assumed for both plates. The distance between the two plates and the nominal density of the flow are chosen so that the body-length global Knudsen number of the flow is 0.01, 0.03, or 0.1. In all three cases ($Kn_{\mathrm{BLG}} = 0.01, 0.03$, and 0.1), 200 computational cells are used with a cell size that is less than the mean free path of the argon gas. The continuum/particle interface is fixed in all three cases so that 70% of the cells are calculated by the N–S approach (see Fig. 4). In order to avoid numerical problems due to the fluctuation of information through the interface, roughly 50 particles per particle cell are used when $Kn_{\mathrm{BLG}} = 0.01$ and more than 500 particles are required when $Kn_{\mathrm{BLG}} = 0.1$. However, it will be shown that the continuum approach is invalid when $Kn_{\mathrm{BLG}} = 0.1$.

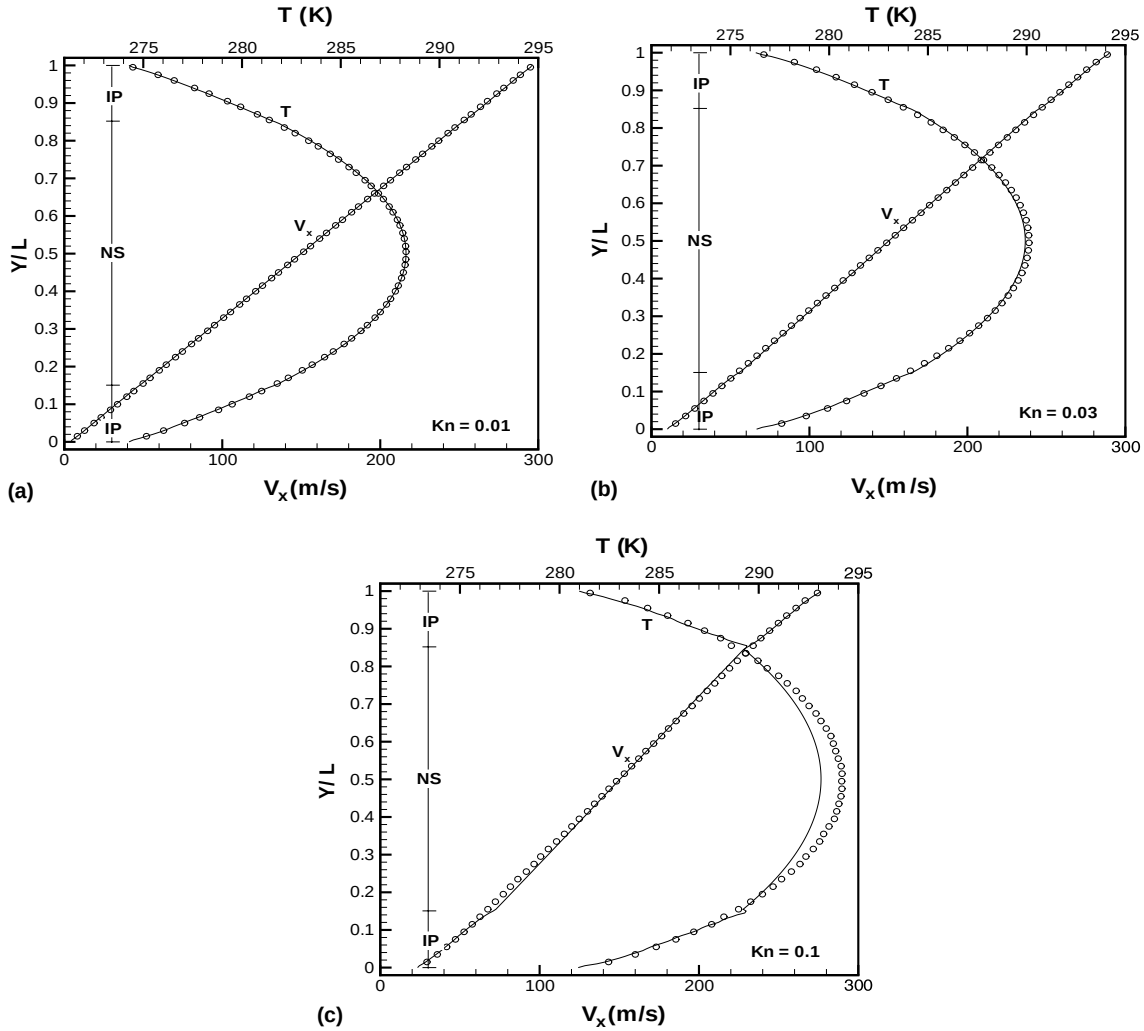

Fig. 4. Comparison of the velocity and temperature distributions obtained using the IP code (circle) and the hybrid code (line): (a) $Kn = 0.01$; (b) $Kn = 0.03$; (c) $Kn = 0.1$.

The results obtained using the hybrid approach are illustrated in Fig. 4, where these results are compared with the results obtained by the IP method only. When $Kn_{\mathrm{BLG}} = 0.01$, excellent agreement between the two results is obtained, which shows the consistency of the hybrid approach and the full IP method. When $Kn_{\mathrm{BLG}} = 0.03$, the smooth results obtained using the hybrid approach demonstrate that the interface is still working well. However, the slight difference between the two temperature results in the continuum domain may indicate that the continuum equations are becoming invalid. When $Kn_{\mathrm{BLG}} = 0.1$, the distorted profiles obtained using the hybrid approach around the interface indicate that the N–S equations are not valid there, which also means it is impossible for continuum equations with slip models to predict the flow under this condition.

Next, typical continuum breakdown parameters are evaluated for this Couette flow. The parameter P, which was proposed for predicting expanding flows [37], fails for this flow because the density does not change along the streamline. Some other parameters are shown with their profiles calculated from the full IP results in Fig. 5. These results show that the gradient-length local Knudsen number also fails because this

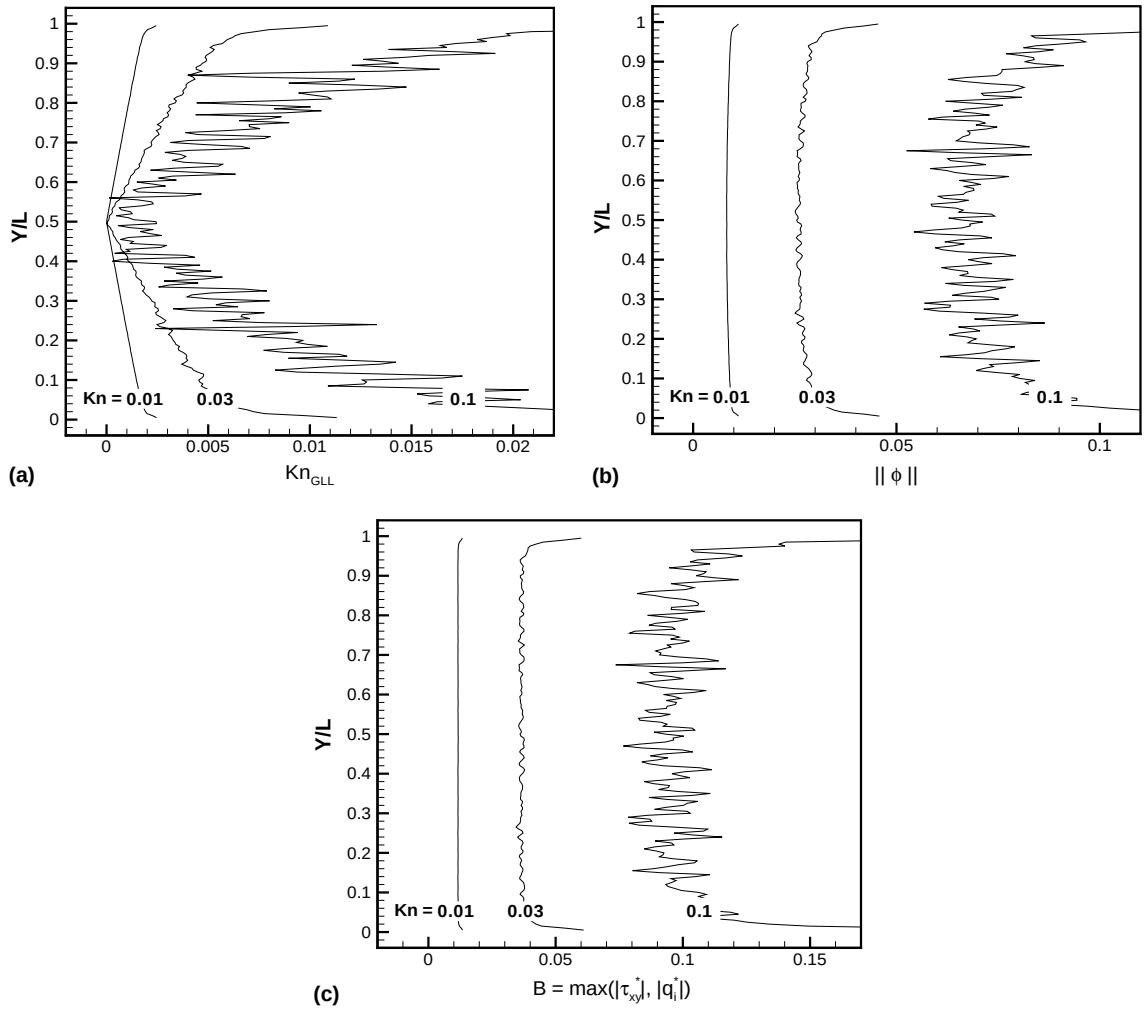

Fig. 5. Profiles of the continuum breakdown parameters (a) Kn_{GLL}, (b) $\|\phi\|$, and (c) B for the Couette flows having various Kn_{BLG}.

parameter is mainly zero (excluding the scatter) around the centerline of the Couette flow. However, the parameters $\|\phi\|$ and B display reasonable behavior, and their values increase when the flow becomes more rarefied. It can be concluded that the cutoff value of these two parameters is on the order of 0.03 for this flow, based on the results illustrated in Fig. 4. However, the cutoff value may vary for different flows.

4.2. Flows over a flat plate

For subsonic external micro-scale gas flows, a hybrid approach is no doubt the best choice for simulations because most of the computational domain can be described by the continuum equations. In this section, an airflow over a flat plate is simulated using the hybrid approach with the second strategy of generating particles through the interface.

The length of the plate is 20 μm and it has a fixed temperature of 295 K. The free stream has a Mach number of 0.2, a temperature of 295 K, and a density of 1.32 kg/m^3. Thus, the Reynolds number of the flow is about 10, and the body-length global Knudsen number is roughly 0.024. In the simulation, full thermal accommodation is assumed for the plate and the VHS molecular model is used. A computational domain is set up having 60 μm in the upstream region, 130 μm in the downstream region and a full span of 120 μm.

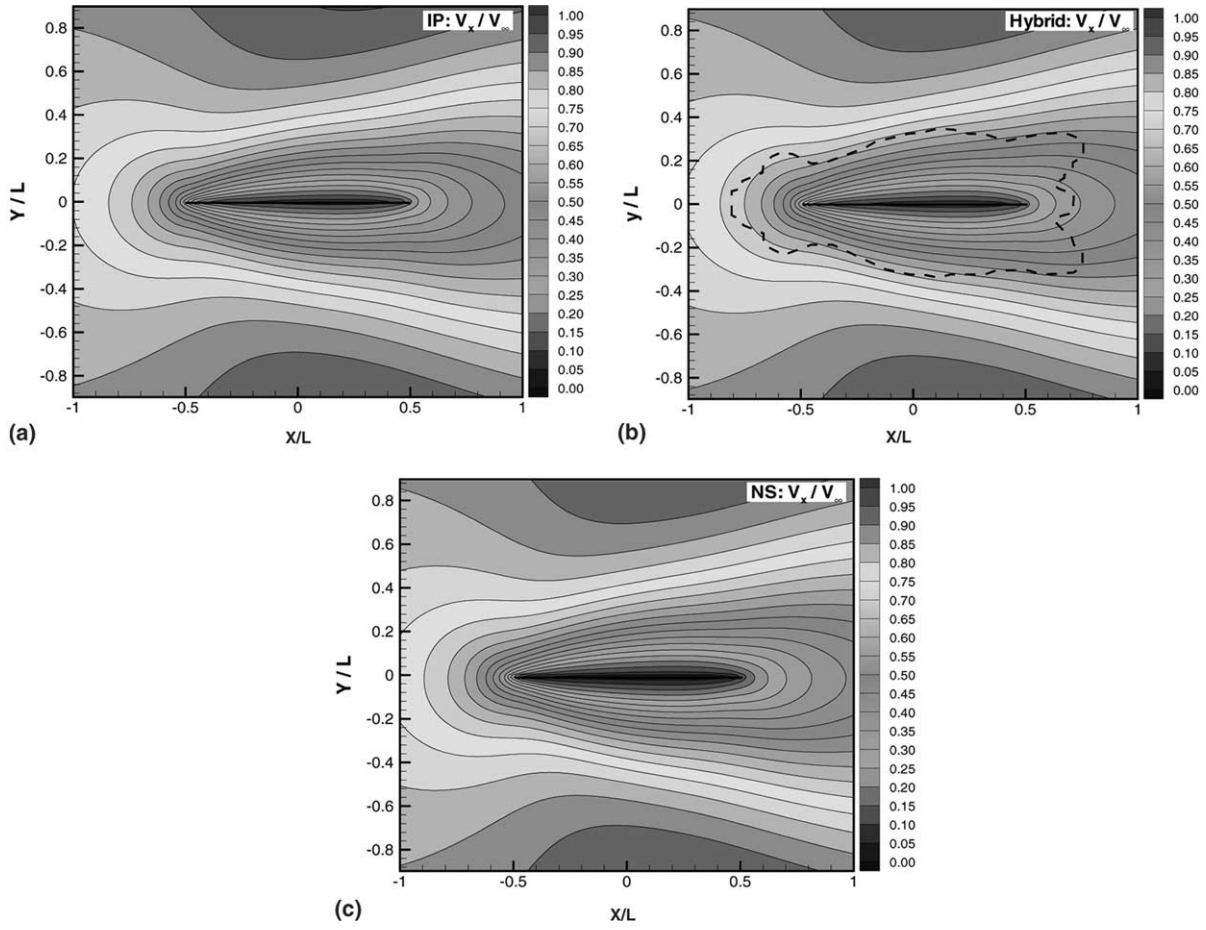

Fig. 6. Comparison of velocity contours from simulations using (a) the full IP, (b) the hybrid, and (c) the full NS configurations.

Characteristic boundary conditions are adopted for the external boundaries. On average, about 20 particles are used for each particle cell, and the time step is less than the mean collision time of the molecules.

With the previous specifications, we simulate the flow using the hybrid approach with different continuum/particle domain configurations. If the entire computational domain is simulated by the IP method, then the full IP method is recovered from the hybrid approach. Similarly, the full N–S approach is used when the entire flow is computed by the continuum approach. Fig. 6 shows a comparison of the parallel velocity contours obtained with different domain configurations. For the hybrid result in this figure, the cutoff value of the parameter B is set to 0.005, and the IP method is used for the domain inside the interface as indicated by the dashed line. The overall agreement among flow field results, e.g., parallel velocity field in Fig. 6, is good because the flow is in the slip regime. However, some differences are shown in Fig. 7 for the surface properties (pressure coefficient, skin friction coefficient, and slip velocity). In the figure, the cutoff value of the parameter B is 0.002 for the results with "hybrid 1", 0.005 for the results with "hybrid 2", and 0.01 for the results with "hybrid 3"; and three levels of buffer cells and three levels of reservoir cells are used. Fig. 7 shows that the surface pressure profiles are very close for all results illustrated. It is also found

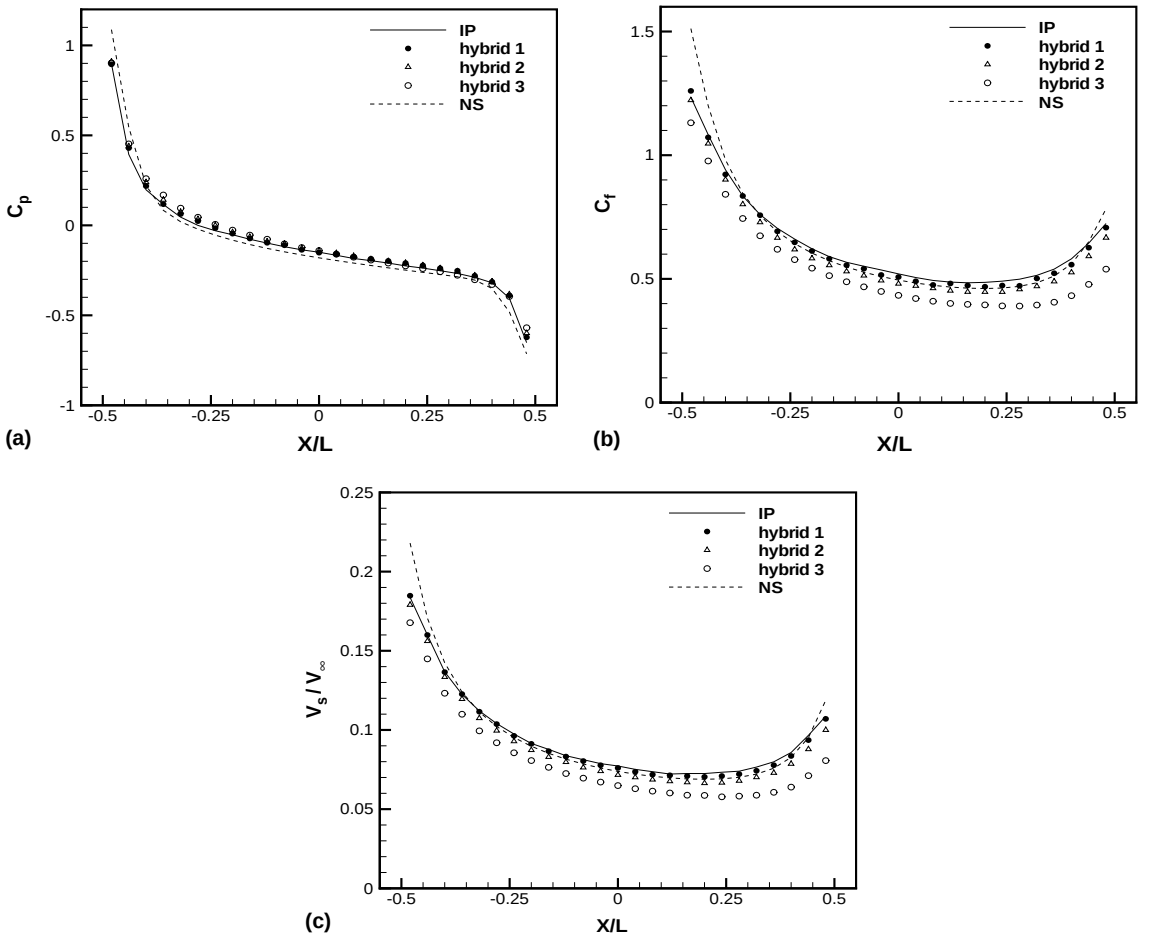

Fig. 7. Comparison of surface properties from simulations with the full IP, the hybrid, and the full NS configurations: (a) pressure coefficient; (b) skin friction coefficient; (c) slip velocity.

that the shear stress and the slip velocity on the surface decrease when the IP domain shrinks. Here, the slip velocity is the flow velocity of the air attached to the plate. The N–S approach, however, predicts larger shear stresses and slip velocities near both ends of the plate, which may indicate the breakdown of the continuum equations in these regions because both ends act as singular points. It should be pointed out that the results of "hybrid 3" seem to be worse than the N–S solution. This is not surprising because the particle domain is too small and a misplacement of the interface does not mean that the solution will be improved. The implementation of the interface will also affect the solution. Hence, it is necessary to apply the hybrid approach with a suitable interface configuration for this kind of flow and more rarefied flows, considering the difference between the "hybrid 1" results and the N–S solution near both ends of the plate.

The implementation of the interface is also investigated. First, the effect of the particle number in each particle cell is investigated. It is found that there is no obvious changes of overall flow field and the surface properties (pressure coefficient, skin friction coefficient, and slip velocity) when the particle number in each cell is increased from 20 to 50, which means that the small statistical scatter of the preserved macroscopic information does not cause problems for the N–S solver to use information from the IP domain. Second, the effect of buffer and reservoir cells is investigated. Fig. 8 shows a comparison of the surface properties

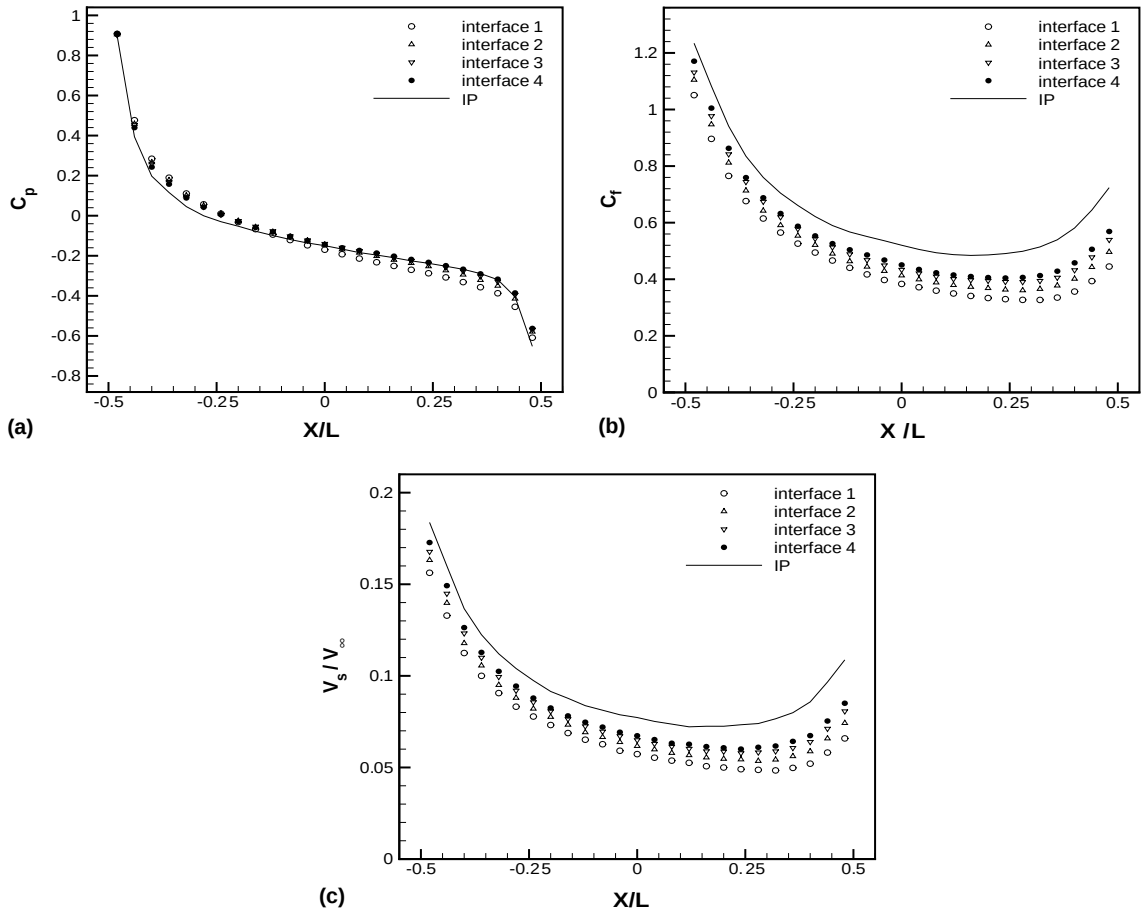

Fig. 8. Comparison of surface properties from simulations with the full IP and the hybrid 3 domain with different buffer and reservoir cells: (a) pressure coefficient; (b) skin friction coefficient; (c) slip velocity.

obtained with different sets of buffer and reservoir cells for the hybrid 3 case. In Fig. 8, the number of levels for the buffer and reservoir cells are: one and two for "interface 1", two and three for "interface 2", three and three for "interface 3", and four and three for "interface 4". Clearly, the results become better when more buffer and reservoir cells are used, which means that the way particles are generated for the reservoir cells is important, especially the preserved macroscopic information of particles should have a distribution because the flow in the reservoir cells is not in an equilibrium state. This is one finding that will help develop future more efficient hybrid schemes.

It seems that 0.002 is an acceptable cutoff value for the continuum breakdown parameter B for the flows over a flat plate using the current hybrid scheme as illustrated in Fig. 6. However, this value for the parameter B is much smaller than the value required for the Couette flow. One main reason for the small cutoff value of B is that the distribution of particles for the reservoir cells is approximate. The cutoff value of B can be increased when a better implementation of the interface is developed. Another possible reason for the change of the cutoff value is that this value depends on the flow problem. If it is assumed that continuum equations begin to break down at locations 10 mean free paths away from the plate (regarding the plate as a disturbance source), then the gradient of flow information around these locations is smaller for a 2D flow problem than for a 1D flow problem. Therefore, the value of B is smaller for a 2D problem than for a 1D problem because B is dependent on gradients of flow information (see Eqs. (15) and (19)).

The flow over the flat plate is also treated as an unsteady flow when the flat plate suddenly obtains a constant parallel velocity in an otherwise still gas. It is simulated in the frame of the flat plate, which means the plate is at rest while the gas has a relative velocity. In order to reduce the numerical fluctuations during the simulation, about 100 particles are simulated in each particle cell. The continuum/particle interface ($B = 0.002$) is adjusted every 10 steps, and the instant flow field is obtained by averaging results over 10 steps. Fig. 9 shows the evolution of the continuum/particle interface and the corresponding velocity flow field. It shows the particle domain is relatively large when the time is small because the flow is limited to a relatively small domain at this early stage and thus the gradients of the flow properties are relatively large. When the time is large enough ($t > 5 \times 10^{-6}$ s), the flow reaches a steady state and the continuum/particle interface remains unchanged except for numerical fluctuations. Clearly, the hybrid simulation saves a lot of computational time because the particle domain changes with time.

4.3. Flow over a micro-scale airfoil

There is interest to study the aerodynamic characteristics of micro-scale airfoils due to the development of micro air vehicles (MAVs) and due to studies of fluid mechanics of tiny insects. Experiments [42] have shown that conventional streamlined airfoils do not perform as well as a flat plate having a thickness ratio of 5% at a low Reynolds number of 4000. Therefore, we are interested to investigate the fluid mechanics of a micro-scale flat plate having a thickness ratio of 5%. As an application of the hybrid approach, we present a case when the angle of attack is 20°.

The length of the plate is 30 μm and it has a fixed temperature of 295 K. The free stream has a Mach number of 0.2, a temperature of 295 K, and a pressure of 1.0 atmosphere. Thus, the Reynolds number of the flow is about 136, and the Knudsen number based on the plate length is close to 0.002. Again, full thermal accommodation is assumed for the plate and the VHS molecular model is used. The computational domain has an area with a radius of 150 μm, and part of the computational grid is shown in Fig. 10. In the figure, the thicker solid line shows the continuum/particle interface, which is fixed in this case. The interface employs three levels of buffer cells and three levels of reservoir cells. The contour of the continuum breakdown parameter B is also shown in the figure. On average, about 100 particles are used for each particle cell, and the time step is less than the mean collision time of the molecules. In this case, the N–S approach is valid only except for a very small part of the computational domain as indicated by the contours of the parameter B in Fig. 10, which is the reason why the hybrid approach is used.

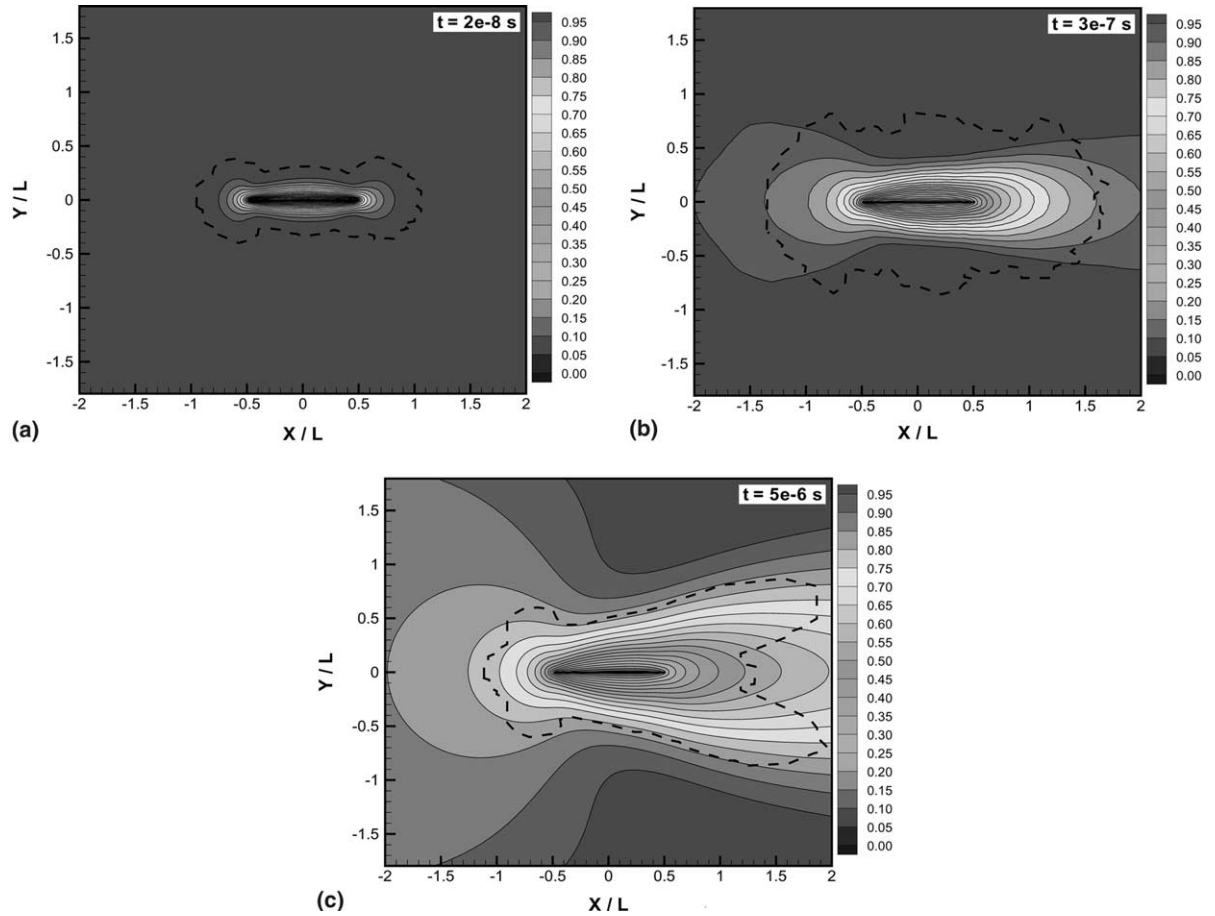

Fig. 9. Evolution of continuum/particle interface (dashed line) and corresponding parallel velocity contours (V_x/V_∞): (a) time $= 2 \times 10^{-8}$ s; (b) time $= 3 \times 10^{-7}$ s; (c) time $= 5 \times 10^{-6}$ s.

The pressure field and some streamlines around the airfoil are shown in Fig. 11. Clearly, the pressure increases when the flow faces the airfoil, and drops when the flow leaves the airfoil, which results in an adverse pressure gradient along the upper side of the airfoil. Due to this adverse pressure gradient and viscous effects, the flow is separated above the airfoil. Careful inspection of the velocity field shows that this separation starts at a location 10% of the plate length downstream of the leading edge of the airfoil. The pressure and skin friction distributions on the airfoil are shown in Figs. 12 and 13, respectively. Based on these data, we calculate a drag coefficient of 0.54 and a lift coefficient of 0.81 (the N–S simulation predicts a drag coefficient of 0.50 and a lift coefficient of 0.78), which are larger than the corresponding coefficients ($C_D = 0.35,\ C_L = 0.74$) when the Reynolds number is 4000. Although these are only the flow properties at one angle of attack, it clearly shows that the aerodynamic characteristics of the 5% flat plate varies with the flow Reynolds number. More details of low Reynolds aerodynamics may be found in [27].

4.4. Numerical performance of the hybrid approach

The objective of a hybrid approach is to reduce the computational cost of an accurate numerical simulation by combining the physical accuracy of kinetic methods and the numerical efficiency of continuum

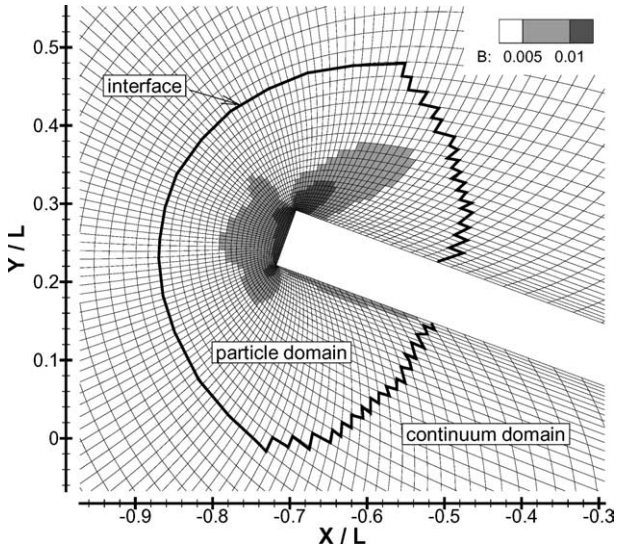

Fig. 10. Part of the computational grid for flow over a micro-scale airfoil.

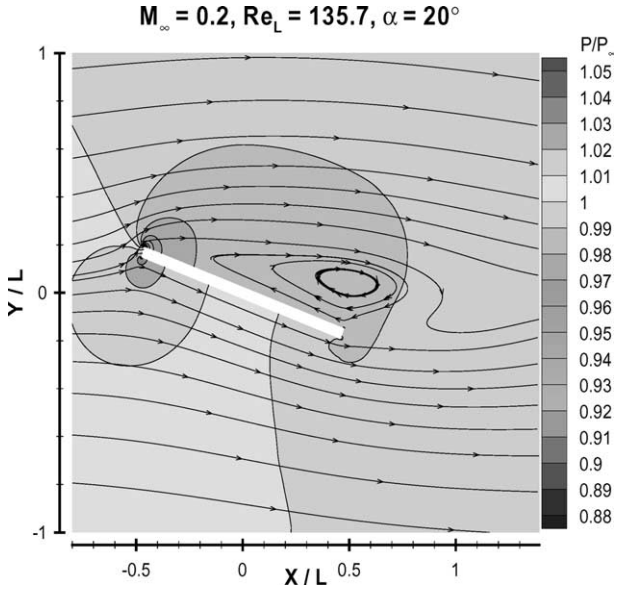

Fig. 11. Pressure field and streamlines for flow over a 5% flat plate.

approaches. Therefore, a basic requirement for a hybrid approach is to consume less computational cost than a kinetic approach when simulating a flow.

The computational cost of a hybrid approach consists of three parts: the cost spent on the particle cells, the cost spent on the continuum cells, and the cost spent on the interface. First, the cost for the particle cells is proportional to the number of particle cells, and depends on the number of simulated particles in each cell. We find that the time for a particle cell in the hybrid approach is almost the same as the time spent on a

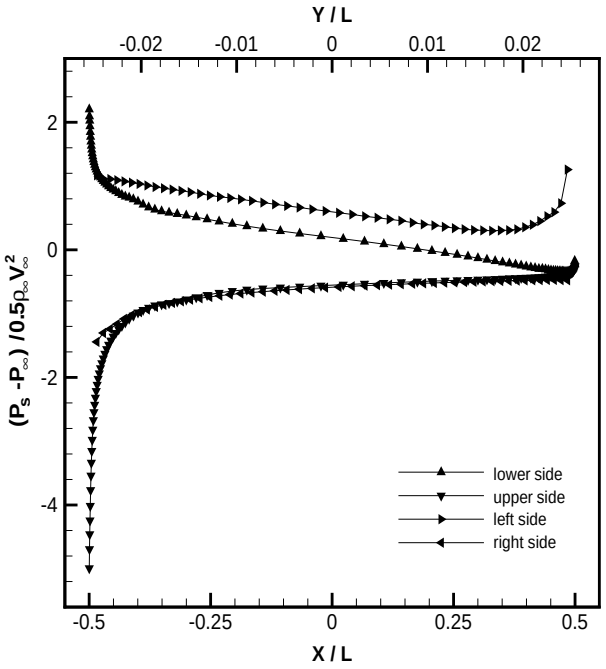

Fig. 12. Distribution of the pressure coefficient along the 5% flat plate having a 20° angle of attack.

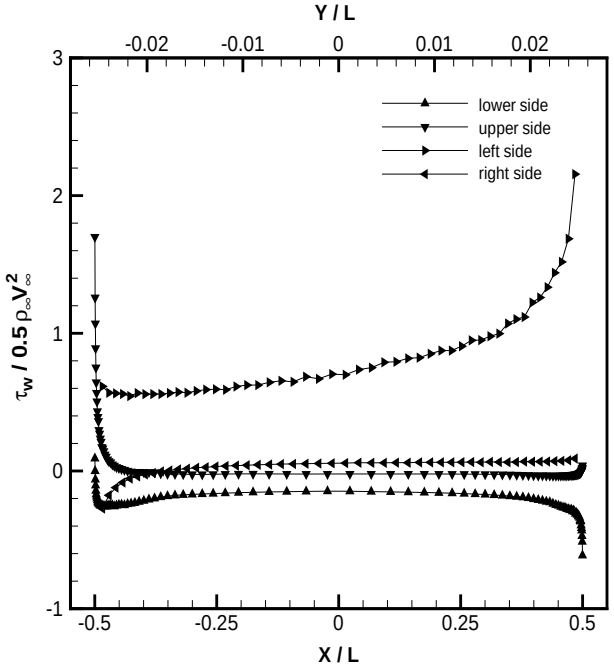

Fig. 13. Distribution of the skin friction coefficient along the 5% flat plate having a 20° angle of attack.

Table 1
Average time spent on one time step on a Pentium 4 PC

Configuration	N_{IP}	N_{NS}	N_{buf}	N_{res}	t_{est} (ms)	t_{real} (ms)
Full NS		18,750			54.7	54.6
Full IP	18,750				328	327
Hybrid 1	3840	14,910	267	545	139	137
Hybrid 2	1454	17,296	148	308	92.0	92.2
Hybrid 3						
Interface 1	540	18,210	74	160	70.9	71.4
Interface 2	540	18,210	152	258	76.5	77.0
Interface 3	540	18,210	234	270	78.5	78.3
Interface 4	540	18,210	320	282	80.5	80.2

cell in the pure IP approach, because the additional variables associated with the hybrid cell only cost a little more computer memory. Second, the cost for the continuum cells is proportional to the number of continuum cells. The cost spent on one continuum cell is only about one sixth of the time spent on a particle cell in which about 20 particles are simulated. This is the reason why more continuum cells are preferred as long as the continuum approach is valid. It should be mentioned that the N–S solver implemented in the MONACO system is less numerically efficient but more powerful than a general solver because the current approach is based on the cell structure which helps solve complicated geometry problems. Third, the cost spent on the interface is more complicated. It depends on the number of buffer cells and the number of reservoir cells. It is found that the time spent on one buffer cell is very close to the time spent on a general particle cell, whereas a reservoir cell requires about two and a half times the time spent on a general particle cell. This is because a large amount of time is spent on redistribution of the particles for the reservoir cells. The average time t_{real} spent on one time step is listed in Table 1 for the case of flow over a flat plate for several hybrid configurations when the hybrid code runs on a Pentium 4 personal computer. In Table 1, we also list the estimated time t_{est} which is evaluated based on Eq. (23), where N_{IP} is the number of IP cells, N_{NS} is the number of N–S cells, N_{buf} is the number of buffer cells, N_{res} is the number of reservoir cells, and $t_{IP} = 17.5$ μs is the time spent on one IP cell.

$$t_{est} = (N_{IP} + N_{NS}/6 + N_{buf} + 2.5N_{res})t_{IP}. \tag{23}$$

Clearly, the numerical performance of the hybrid approach depends on the number ratio of the particle cells to the continuum cells and on the number percentage of the buffer cells and the reservoir cells. For example, the hybrid 3 case, a hybrid simulation costs about 50% more than a pure N–S simulation, but about a factor of 3 less than a full IP simulation. Thus, it is better to apply the hybrid approach to flows in which most of the flow domain can be described by continuum equations.

5. Concluding remarks

We have proposed a hybrid approach by coupling the information preservation (IP) method and a N–S approach for subsonic, rarefied gas flows. The particle domain and the continuum domain were separated by a continuum/particle interface, and information was exchanged through the interface at every time step. The interface was adaptively determined by a continuum breakdown parameter so that the maximum benefits from hybrid schemes can be obtained. The N–S approach can directly use the information from the IP method because the IP method preserved the macroscopic information at every time step. Schemes for generating particles through the interface were investigated. Our new scheme with the use of the buffer and reservoir cells worked better than the Marshak-type scheme. Simulation of a flow over a flat plate showed

the ability of the hybrid approach and revealed the effects of the cutoff value of the continuum breakdown parameter suggested by Garcia et al.. We also applied the hybrid approach to study the aerodynamic characteristics of a micro-scale airfoil. The hybrid approach generally spent less computational time than the IP method for rarefied gas flows, and the numerical performance of the hybrid approach depended on the number ratio of continuum cells to particle cells.

Acknowledgements

The authors greatly appreciate the support from the Air Force Office of Scientific Research through MURI grant F49620-98-1-0433.

References

[1] S.D. Senturia, Microsystem Design, Kluwer Academic Publishers, Norwell, 2000.
[2] Q. Sun, I.D. Boyd, G.V. Candler, Numerical simulation of gas flow over microscale airfoils, Journal of Thermophysics and Heat Transfer 16 (2) (2002) 171.
[3] W.-L. Wang, I.D. Boyd, Predicting continuum breakdown in hypersonic viscous flows, Physics of Fluids 15 (1) (2003) 91.
[4] C. Hirsch, Numerical Computation of Internal and External Flows I & II, Wiley, Chichester, 1990.
[5] G.E. Karniadakis, A. Beskok, Micro Flows: Fundamentals and Simulation, Springer, New York, 2001.
[6] M. Gad-el-Hak, The fluid mechanics of microdevices – the freeman scholar lecture, Journal of Fluids Engineering 121 (1999) 5.
[7] G.A. Bird, Molecular Gas Dynamics and the Direct Simulation of Gas Flows, Oxford University Press, New York, 1994.
[8] D.B. Hash, H.A. Hassan, A decoupled DSMC/Navier–Stokes analysis of a transitional flow experiment, AIAA paper 96-0353 (1996).
[9] F.E. Lumpkin, P.C. Stuart, G.J. Lebeau, Enhanced analyses of plume impingement during Shuttle-Mir docking using a combined CFD and DSMC methodology, AIAA paper 96-1877 (1996).
[10] J.F. Bourgat, P.L. Tallec, M.D. Tidriri, Coupling Boltzmann and Navier–Stokes equations by friction, Journal of Computational Physics 127 (1996) 227.
[11] C.K. Oh, E.S. Oran, A new hybrid algorithm: Navier–Stokes as a DSMC filter, AIAA paper 98-0849 (1998).
[12] D.C. Wadsworth, D.A. Erwin, One-dimensional hybrid continuum/particle simulation approach for rarefied hypersonic flows, AIAA paper 90-1690 (1990).
[13] D.C. Wadsworth, D.A. Erwin, Two-dimensional hybrid continuum/particle approach for rarefied flows, AIAA paper 92-2975 (1992).
[14] D.B. Hash, H.A. Hassan, Assessment of schemes for coupling Monte Carlo and Navier–Stokes solution methods, Journal of Thermophysics and Heat Transfer 10 (1996) 242.
[15] D.B. Hash, H.A. Hassan, Two-dimensional coupling issues of hybrid DSMC/Navier–Stokes solvers, AIAA paper 97-2507 (1997).
[16] R. Roveda, D.B. Goldstein, P.L. Varghese, Hybrid Euler/particle approach for continuum/rarefied flows, Journal of Spacecraft and Rockets 35 (3) (1998) 8.
[17] R. Roveda, D.B. Goldstein, P.L. Varghese, Hybrid Euler/direct simulation Monte Carlo calculation of unsteady slit flow, Journal of Spacecraft and Rockets 37 (6) (2000) 753.
[18] P.L. Tallec, F. Mallinger, Coupling Boltzmann and Navier–Stokes equations by half fluxes, Journal of Computational Physics 136 (1997) 51.
[19] A.L. Garcia, J.B. Bell, W.Y. Crutchfield, B.J. Alder, Adaptive mesh and algorithm refinement using direct simulation Monte Carlo, Journal of Computational Physics 154 (1999) 134.
[20] N.G. Hadjiconstantinou, Hybrid atomistic-continuum formulations and the moving contact-line problem, Journal of Computational Physics 154 (1999) 245.
[21] O. Aktas, N.R. Aluru, A combined continuum/DSMC technique for multiscale analysis of microfluidics filters, Journal of Computational Physics 178 (2002) 342.
[22] E.G. Flekkøy, G. Wagner, J. Feder, Hybrid model for combined particle and continuum dynamics, Europhysics Letters 52 (2) (2000) 271.
[23] B. Alder, Highly discretized dynamics, Physica A 240 (1997) 193.
[24] S. Tiwari, A. Klar, An adaptive domain decomposition procedure for Boltzmann and Euler equations, Journal of Computational and Applied Mathematics 90 (1998) 223.

[25] J. Fan, C. Shen, Statistical simulation of low-speed rarefied gas flows, Journal of Computational Physics 167 (2001) 393.
[26] Q. Sun, I.D. Boyd, A direct simulation method for subsonic, microscale gas flows, Journal of Computational Physics 179 (2002) 400.
[27] Q. Sun, Information preservation methods for modeling micro-scale gas flows, PhD Dissertation, University of Michigan, Ann Arbor, 2003.
[28] W.-L. Wang, I.D. Boyd, A new energy flux model in the DSMC-IP method for nonequilibrium flows, AIAA paper 2003-3774 (2003).
[29] C. Cai, I.D. Boyd, J. Fan, G.V. Candler, Direct simulation methods for low-speed microchannel flows, Journal of Thermophysics and Heat Transfer 14 (3) (2000) 368.
[30] J. Fan, I.D. Boyd, C. Cai, K. Hennighausen, G.V. Candler, Computation of rarefied flows around a NACA0012 airfoil, AIAA Journal 39 (4) (2001) 618.
[31] R.P. Nance, D.B. Hash, H.A. Hassan, Role of boundary conditions in Monte Carlo simulation of MEMS devices, Journal of Thermophysics and Heat Transfer 12 (3) (1998) 447.
[32] K. Guo, G.S. Liaw, A review: boundary conditions for the DSMC method, AIAA paper 2002-2953 (2001).
[33] R.W. MacCormack, G.V. Candler, The solution of Navier–Stokes equations using Gauss–Seidel line relaxation, Computers & Fluids 17 (1989) 135.
[34] K. Hennighausen, Fluid mechanics of microscale flight, PhD Dissertation, University of Minnesota, Minneapolis, 2001.
[35] S.A. Schaaf, P.L. Chambre, Flow of rarefied gases, High Speed Aerodynamics and Jet Propulsion 3 (H) (1958) 678.
[36] S. Chapman, T.G. Cowling, The Mathematical Theory of Non-Uniform Gases, third ed., Cambridge University Press, Cambridge, 1970.
[37] G.A. Bird, Breakdown of translational and rotational equilibrium in gaseous expansions, AIAA Journal 8 (1970) 1998.
[38] I.D. Boyd, G. Chen, G.V. Candler, Predicting failure of the continuum fluid equations in transitional hypersonic flows, Physics of Fluids 7 (1995) 210.
[39] S. Tiwari, Coupling the Boltzmann and Euler equations with automatic domain decomposition, Journal of Computational Physics 144 (1998) 710.
[40] A.L. Garcia, B.J. Alder, Generation of the Chapman–Enskog distribution, Journal of Computational Physics 140 (1998) 66.
[41] S. Dietrich, I.D. Boyd, Scalar and parallel optimized implementation of the direct simulation Monte Carlo method, Journal of Computational Physics 126 (1996) 328.
[42] S. Sunada, A. Sakaguchi, K. Jawachi, Airfoil section characteristics at a low Reynolds number, Journal of Fluids Engineering 119 (1997) 129.